*energies*

*Review*

# 3D-Printable Concrete for Energy-Efficient Buildings

**Manideep Samudrala [1], Syed Mujeeb [1], Bhagyashri A. Lanjewar [1], Ravijanya Chippagiri [1], Muralidhar Kamath [2] and Rahul V. Ralegaonkar [1,*]**

[1] Department of Civil Engineering, Visvesvaraya National Institute of Technology, Nagpur 440010, India; mt21ctm006@students.vnit.ac.in (M.S.); mt21ctm016@students.vnit.ac.in (S.M.); dt21civ012@students.vnit.ac.in (B.A.L.); ravijanya991@students.vnit.ac.in (R.C.)

[2] General Manager Technical Services, Apple Chemie India Private Limited, Nagpur 440022, India; sales@applechemie.com

* Correspondence: rvralegaonkar@civ.vnit.ac.in

**Abstract:** Rapid construction with an energy-efficient approach is a major challenge in the present construction industry. Cement, a carbon-intensive material, is mainly used in the construction industry and hence increases the sector's carbon footprint on the environment. The current review focuses on the study of 3D concrete printing (3DCP), in which cement is partially replaced with industrial byproducts such as ground granulated blast furnace slag (GGBS), fly ash, and silica fume. Walling material is primarily targeted in 3DCP. There is a need to include energy efficiency to achieve a thermally comfortable environment. The life cycle assessment (LCA) of concrete is studied to discover the potential conflicts affecting the environment. The sand-to-binder ratio is pivotal in determining the performance of concrete. The content of the supplements is decided based on this factor. The rheological, physical, and mechanical properties of 3DCP are studied further and analysed. GGBS demonstrates better performance in the compressive and flexure strength of concrete. The usage of fly ash and silica fume has reduced the thermal conductivity of the material, whereas GGBS has increased it. An LCA study shows that 3DCP can be made sustainable with the use of these supplementary cementitious materials.

**Keywords:** 3DCP; energy efficiency; life cycle assessment; industrial byproducts

check for updates

**Citation:** Samudrala, M.; Mujeeb, S.; Lanjewar, B.A.; Chippagiri, R.; Kamath, M.; Ralegaonkar, R.V. 3D-Printable Concrete for Energy-Efficient Buildings. *Energies* **2023**, *16*, 4234. https://doi.org/10.3390/en16104234

Academic Editor: Alessia Arteconi

Received: 8 April 2023
Revised: 18 May 2023
Accepted: 19 May 2023
Published: 21 May 2023



## 1. Introduction

In this era of rapid urbanization, faster construction has become a major issue. Three-dimensional concrete printing (3DCP) utilizes a 3D printer that allows concrete to print in layers and in the required geometry. Three-dimensional concrete has greater potential value in the present construction industry [1]. It helps in building structures without the use of formwork and thereby reduces the construction cost. Three-dimensional concrete printing helps to complete construction with high accuracy and low-cost building components, and it facilitates easy remote-area construction [2]. In recent years, 3DCP has gained attention in the global construction sector due to its ability to facilitate faster construction. This technology helps in the reduction of the labor force and of wastage during the construction phase. It directly reduces the total cost of construction by making the construction sustainable [3,4].

An important aspect of 3D concrete printing is the machine that prints the structure. A 3D printer uses a Cartesian coordinate system for printing the structures. A printer has been designed with a mini bed size of 1 m × 1 m × 1 m [5]. The entire motion of the printer is controlled using software that includes a G-code as input, which controls the nozzle motion.

The 3D printer has a gantry crane to which the nozzle is attached. Concrete is allowed to fall through this nozzle [6]. An Italian civil engineer built a D-shaped 3D printer that prints layers of a thickness of 5–10 mm [7]. The extrusion nozzle plays an important role in determining the shape stability of the printed concrete. Nozzles have different shapes such as circles, rectangles, U-shapes, and inverted U-shapes [8]. These move with different speeds ranging from 10 mm/s to 100 mm/s and it has been demonstrated that the nozzle with a 15 mm diameter releases concrete smoothly [9]. A screw-type nozzle is preferred to control the extrusion speed [10]. For better consistency, the nozzle lift should be the same as the thickness of the printed layers [11]. The layer width is increased linearly with increased extrusion velocity, and printability is increased at lower printing speed. Figure 1 shows a laboratory-scale 3D printing system.

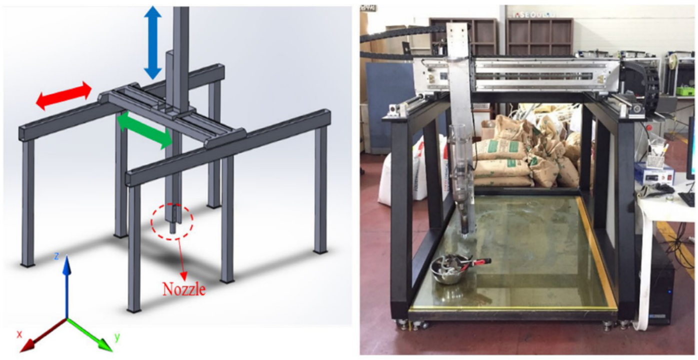


**Figure 1.** Laboratory-scale 3D printing system [5].

Larger quantities of cement are used in 3D concrete to accommodate the strength lost due to the elimination of coarse aggregate and to maintain rheology. This has led to an increase in energy content and the carbon footprint on the built structure. Energy efficiency and thermal performance also play a major role in the design of concrete. Wall structures play a key role in the energy efficiency of a building or structure. Three-dimensional concrete printing is mainly used as a walling material, owing to which thermal performance is a major issue in the design of 3D concrete. Consequently, there is a need to incorporate supplements for cement in the concrete that reduce the quantity of cement while maintaining the necessary thermal comfort [12,13]. Ground granulated blast furnace slag (GGBS), fly ash, and silica fume are some known industrial byproducts that are used as a partial replacement for cement [14,15]. Different tests regarding the physical and chemical properties of the materials that are used have been performed [16,17]. Based on the results obtained, the usage of these materials in the mix is controlled [18]. The addition of cementitious supplements is performed stage-wise and their effect on the physical properties of the concrete is noted down. A mega-scale 3D printing system is required to print the concrete and to check its different properties.

The present literature focuses on the study of the partial substitution of cement with cementitious supplements such as GGBS, fly ash, and silica fume along with the 3D printing system and its nozzle requirements. The impact of rheological, physico-mechanical, and thermal properties, along with the technical challenges faced, is studied to check the suitability of 3D-printable concrete in energy-efficient buildings.

## 2. Materials and Methods

### 2.1. Materials

Raw material characteristics play an important role in defining the physical, chemical, and mechanical properties of 3D concrete. Raw material characterization includes finding particle size distribution, specific gravity, density, and morphology. Chemical characteristics consist of the chemical composition of materials and their reactivity. X-ray diffraction (XRD), X-ray fluorescence (XRF), and scanning electron microscopy (SEM) are performed to determine the mineralogy, chemical composition, and morphology of the material, respectively.

#### 2.1.1. Alternative Materials Studied for the Replacement of Cement

Cement is the most used building material in the manufacturing of concrete. Various grades of commercially available ordinary Portland cement (OPC) and Portland pozzolana cement (PPC) are most commonly used. Ordinary Portland cement is used in the development of 3D concrete. As cement plays a major role in the strength of concrete, it should be replaced with an optimum content of industrial byproduct complying with the desired strength. Table 1 shows the chemical composition of cement from various sources by percentage.

**Table 1.** Chemical composition of cement (OPC 53).

| Composition | [19] (%) | [20] (%) | [21] (%) | [22] (%) |
|---|---|---|---|---|
| CaO | 58.02 | 64.85 | 64.2 | 64.7 |
| $SiO_2$ | 23.148 | 21.65 | 20.4 | 20.4 |
| $Fe_2O_3$ | 3.56 | 4.32 | 3.2 | 3.38 |
| $Al_2O_3$ | 9.31 | 5.56 | 4.9 | 4.7 |
| MgO | 1.36 | 0.84 | 1.82 | 0.87 |
| $SO_3$ | 2.62 | 2.58 | 2.58 | 1.89 |
| $K_2O$ | 1.02 | 0.76 | 0.38 | 0.49 |
| $Na_2O$ | 0.411 | 0.24 | 0.24 | 0.33 |

#### 2.1.2. GGBS

Ground granulated blast furnace slag (GGBS) is used as a partial substitution for cement due to its pozzolanic properties. Pig iron manufacturing, a step in the production of steel, produces blast furnace slag as a byproduct (Figure 2). According to estimates, each tonne of pig iron produces approximately 300 kg of slag. It has a similar particle size distribution as cementitious materials [23]. Some 35–50% of it can be used to replace cement, beyond which there is a reduction in the strength of the concrete [24]. As 3DCP requires high resistance to the environment, GGBS provides better chloride resistance [25]. Early age cracking resistance is also achieved [24]. Compared to fly ash, GGBS enhances the strength of concrete [26].

**Figure 2.** Ground granulated blast furnace slag.

The extensive usage of GGBS as a cement substitute in today's concrete is a result of its technological, financial, and environmental benefits. Its use in binary and ternary blended cement concretes is widely claimed to improve mechanical characteristics, resistance to corrosion, and chloride ion penetration. Additionally, it has been demonstrated that well-proportioned, well-curing slag concretes prevent harmful alkali–silica interactions and increase sulphate resistance. The pozzolanic action of slag and microaggregate filling are factors that contribute to the higher performance of GGBS concrete. Its strength development is similar to that of conventional plain cement concrete from 56 days. Table 2 shows the presence of abundant CaO and $SiO_2$ in the material, making it suitable for the replacement of cement.

**Table 2.** Chemical composition of GGBS (%).

| CaO | $SiO_2$ | $Al_2O_3$ | $Fe_2O_3$ | MgO | $Na_2O$ | $SO_3$ | $TiO_2$ | $K_2O$ | Carbon | Ref |
|---|---|---|---|---|---|---|---|---|---|---|
| 39.37 | 29.65 | 15.56 | 0.35 | 7.54 | 0–1.04 | 4.32 | 0–1.04 | 0–1.04 | 0 | [23] |
| 34.8 | 37.5 | 6.4 | 0.51 | 8.6 | 0.38 | 0 | 0 | 0.9 | 0 | [27] |
| 37.73 | 34.62 | 11.82 | 2.73 | 9.43 | 0.35 | 1.42 | 0 | 0.5 | 0 | [25] |

### 2.1.3. Fly Ash

Fly ash is a pozzolanic material, shown in Figure 3, that is widely used in the construction industry as a replacement for cement. It can replace cement by 25–40% [28,29], but the setting time of concrete increases as the fly-ash content is increased [30]. There is an increased performance in buildability and smoothness in the end product as fly-ash content is increased up to 35% [31]. Table 3 shows the chemical composition of fly ash.

**Figure 3.** Fly ash.

**Table 3.** Chemical composition of fly ash (%).

| CaO | $SiO_2$ | $Al_2O_3$ | $Fe_2O_3$ | MgO | $Na_2O$ | $SO_3$ | $TiO_2$ | $K_2O$ | Carbon | Ref |
|---|---|---|---|---|---|---|---|---|---|---|
| 3.10 | 36.10 | 25.03 | 8.66 | 1.24 | 0 | 0.59 | 0.91 | 1.08 | 23.29 | [32] |
| 2.61 | 52.11 | 23.59 | 7.39 | 0.78 | 0–1.2 | 0 | 0 | 0–1.2 | 0 | [33] |
| 0.6–9 | 50.2–59.7 | 14–32.4 | 2.7–16.6 | 0.1–2.3 | 0.2–1.2 | 0 | 0.3–2.7 | 0.2–4.7 | 0 | [34] |

From Tables 2 and 3, it is seen that GGBS is a better fit for the partial replacement of cement than fly ash, based on its chemical composition. Cement with GGBS has higher early age strength than the cement mix with fly ash; this is a necessary property in 3DCP [35]. Fly ash produces less calcium hydroxide as compared to GGBS, which improves the property of durability. Early age hydration is more prevalent in GGBS-based concrete mix as compared to fly-ash-based mix [35]. Both of these are used as a soil stabilizing agent [36], which is helpful for foundation works in 3DCP.

### 2.1.4. Silica Fume

Silica fume, shown in Figure 4, is another pozzolanic material used as a partial replacement for cement. It can replace cement by 10–15%, beyond which there is a reduction in the compressive strength of the concrete [37–39]. The use of silica fume results in an increased yield stress of up to 1.25 kPa and increased buildability [40]. The tensile strength of concrete represents the bond strength and is improved with the addition of silica fume [38]. Table 4 presents the chemical composition of silica fume.

**Figure 4.** Silica fume.

**Table 4.** Chemical composition of silica fume (%).

| CaO | $SiO_2$ | $Al_2O_3$ | $Fe_2O_3$ | MgO | $Na_2O$ | $SO_3$ | $TiO_2$ | $K_2O$ | Carbon | Ref |
|---|---|---|---|---|---|---|---|---|---|---|
| 0.1–0.5 | 86–96 | 0.4–1 | 0.1–1.5 | 0.3–2 | 0.4–0.5 | 0.1–0.4 | 0 | 0.3–3 | 0.5–2.5 | [41] |
| 0.69 | 93.35 | 0.92 | 0.71 | 0.72 | 0.33 | 0.13 | 0 | 0.86 | 0 | [42] |
| 0.94 | 92.6 | 0.89 | 1.97 | 0.96 | 0 | 0.33 | 0.25 | 1.31 | 0.07 | [43] |

From the above Tables, it is inferred that GGBS and fly ash are superior to silica fume, based on the chemical composition. The compositions of these raw materials are in accordance with Indian standards, and they can be used as supplementary cementitious materials. The use of these materials in 3D printing technology and their behavior for various properties are studied before filling them into the equipment [44]. GGBS has higher bulk density and specific gravity compared to fly ash and silica fume [45].

#### 2.1.5. Aggregate

Concrete constitutes both coarse and fine aggregates. From the study, it is known that coarse aggregates contribute up to 34% of the strength of concrete [46]. As the coarse aggregates are completely eliminated in the making of 3D concrete, there is an increase in the content of fine aggregate. To overcome the strength, there will be an increase in the content of cement. There is a significant impact of sand-to-binder ratio in the making of concrete. Usually, the range of the sand-to-binder ratio lies between 1.1 and 1.7 [47].

### *2.2. Methodology*

To proceed with the review, various methodologies were studied. From the point of selection of raw materials to the end product printing, a sequence of steps is followed. There are three basic parameters that are considered in creating the mix design [48]. They are water-to-binder ratio (w/b), sand-to-binder ratio (s/b), and additive-to-binder ratio. The compressive strength and smoothness of concrete are highly affected by the s/b ratio. The lower the s/b, the higher the strength of concrete [49]. The water-to-binder ratio also affects the strength of the concrete [50]. Researchers have found that 3DCP works well for s/b ratios between 1.1 and 1.6 [47]. Initially, it is fixed, as it decides the strength and finish of 3D concrete. Then, additives are taken out and replaced with cement or fine aggregate at small intervals (e.g., 0%,5%,10%,15%, etc.). Superplasticizer is added to reduce the quantity of water in the mix. A subsequent increase in the strength of the concrete is seen [51]. A slump flow test is conducted simultaneously [3,51]. The optimum mix is then considered for further replacement of fine aggregate.

Then, in the mix described above, fine aggregate substitute or additive is partially replaced with sand at the defined intervals. Slump flow values are to be checked subsequently. A viscosity modifying agent (VMA) and superplasticizer are added to improve the workability and buildability of the concrete.

Mix Procedure and Design

Suitable mixing and casting procedures are adopted to prepare the concrete mix. Materials of the required content are fed into the mixer, and mixing is carried out for homogeneity. Water combined with superplasticizer is added to the mix. The VMA is added to the mix along with water if it is in gel form, or it is sprinkled over the mix if it is in dry form [52].

Initially, the mixing can be started with any water/binder ratio [53]. Then, the mix should be checked for its flowability while simultaneously using flow table apparatus, which in turn shows its workability. If the mix appears dry, then the water/binder ratio is increased to achieve sufficient workability. Superplasticizer is added to the mix to reduce the quantity of water, which in turn reduces the water/binder ratio. By following the above procedure, several trials are carried out to find the optimum mix.

The finalized mix is tested for several rheological properties such as workability, thixotropic open time, extrudability, and buildability by making a sample slab with dimensions of 350 × 350 × 120 mm. Hardened properties, such as compressive strength and flexure strength, are also measured [54].

Concrete made by applying the above mixing procedure requires a target compressive strength and flexure strength with a moderate setting time. Workability and the maximization of buildability are also governing factors in this procedure [51]. By performing various tests, the water/binder range and the sand/binder ratio for concrete with acceptable printable regions are measured [55]. All the rheological properties are to be tested in order, as shown in Figure 5, before finalizing the mix.

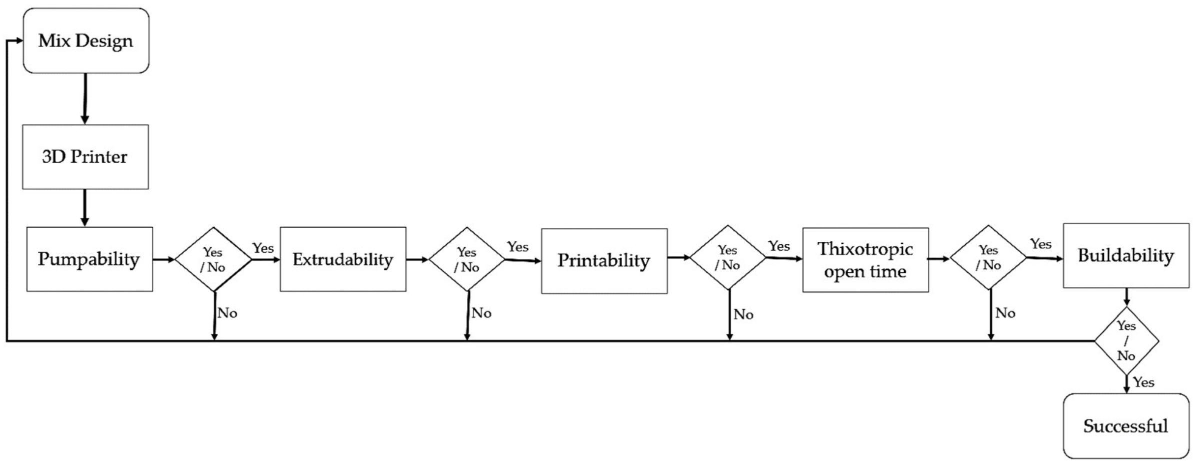


**Figure 5.** Rheological properties testing [47].

Some mix proportions which were used to replace cement and aggregates at various intervals of mixing are shown in Table 5.

**Table 5.** Quantity of materials per m$^3$.

| Cement (kg) | GGBS (kg) | Silica Fume (kg) | Limestone Sand (kg) | Aggregate (kg) | Water (kg) | Superplasticizer (kg) | VMA (kg) | Recycled Sand (kg) | Fibres (kg) | Ref |
|---|---|---|---|---|---|---|---|---|---|---|
| 483 | 314 | 70 | 447 | 284 | 347 | 3.47 | 5.2 | - | - | [56] |
| 458 | 377 | 51 | 195 | 549 | 355 | 2.66 | 2.66 | - | - | |
| 1000 | 0 | 0 | 0 | 1000 | 350 | 1.12 | 1.28 | - | 20 | [57] |
| 1000 | 0 | 0 | 0 | 1000 | 420 | 0.86 | 1.28 | 500 | 5 | |
| 1000 | 0 | 0 | 0 | 1000 | 420 | 1 | 1.28 | 500 | 10 | |
| 1000 | 0 | 0 | 0 | 1000 | 420 | 1.24 | 1.28 | 500 | 20 | |
| 1000 | 0 | 0 | 0 | 1000 | 420 | 2.18 | 1.28 | 500 | 28 | |
| 815 | 0 | 0 | 0 | 1222 | 285 | 4.24 | 0.81 | - | - | [58] |
| 815 | 0 | 0 | 0 | 1222 | 285 | 2.85 | 0.81 | - | - | |

## 3. Rheological Properties of Fresh Concrete

Another key aspect in the success of the 3D-printable concrete lies in its fresh concrete properties. The fresh concrete that is taken for printing should possess rheological properties such as pumpability, extrudability, printability, thixotropy open time, buildability, and setting time [4]. Different tests are performed to find the rheological properties of fresh concrete. As there is no standard procedure for testing these rheological properties, results are obtained by using any appropriate method.

Flowability is the property of fresh concrete that allows the material to move smoothly from the extrusion nozzle. A flowability test is performed by using flow table apparatus, and the flow value is noted. Segregation or bleeding creates difficulty in printing the concrete. Stiff concrete creates an extra demand on the pump, which causes failure in the machine. From the obtained results, it is known that the material with a higher yield stress has less flowability [59]. Flowability also depends on the presence of the optimum aggregate content in the concrete [60].

Extrudability is the ability of the fresh concrete to pump out from the nozzle smoothly without clogging the nozzle. It is also defined as the ability of the concrete to print continuously without any breakage [61,62]. Printing becomes easier only if the concrete is sufficiently extrudable.

Buildability is defined as the ability of fresh printable concrete to exist in the form of bonded layers that bear the load of the newly printed concrete without collapsing [55,62]. It can be related to the green strength of the concrete. The higher the green strength, the higher the ability of the fresh concrete to bear the load, which directly increases its buildability. The test establishes the number of layers that can be printed without collapse. The buildability of 3DCP is improved by using different kinds of admixtures and by active rheological control [63].

Printability is defined as the ability to design the end product or the structure to its desired shape and architecture [64]. It is the difference in the original design and the end geometry that is obtained from printing. Three-dimensional concrete printing is highly prized for its flexibility in creating complex geometries that are difficult to obtain using conventional methods [48,65].

Thixotropy open time (TOT) is defined as the time taken to clog the nozzle from extruding the concrete [66]. It is the time taken by the concrete to lose its extrudability property. It indirectly depends on the setting time of the concrete: the higher the setting time, the higher the thixotropy open time.

Studies show that there is no relationship between yield stress and thixotropy. A minimum of 10,000 N mm rpm of thixotropic value is necessary for 3DCP [67]. All the above rheological properties that are studied are interlinked with the mix design of the concrete.

## 4. Tests on Physico-Mechanical Properties and Testing Procedure

Different physical and mechanical tests are conducted before finalizing the mix and proceeding to end printing. The tests conducted are as follows.

Compressive strength is the main characteristic property of the concrete. Cubes of 100 mm are made and are tested under a compression testing machine [68] for 7 days, 14 days, and 28 days, respectively. The concrete is printed in layers with dimensions of 50 mm × 40 mm × 20 mm and tested [69]. There is an anisotropic behavior in the calculation of the compressive strength of concrete with a fly ash-based mix [70].

From the above-studied material properties, it has been found that the mix with GGBS has a higher compressive strength as compared to other additives.

Various sources have presented different mix designs. The correlation of compressive strength with variation in the binder and superplasticizer properties is indicated in Figures 6 and 7, respectively.

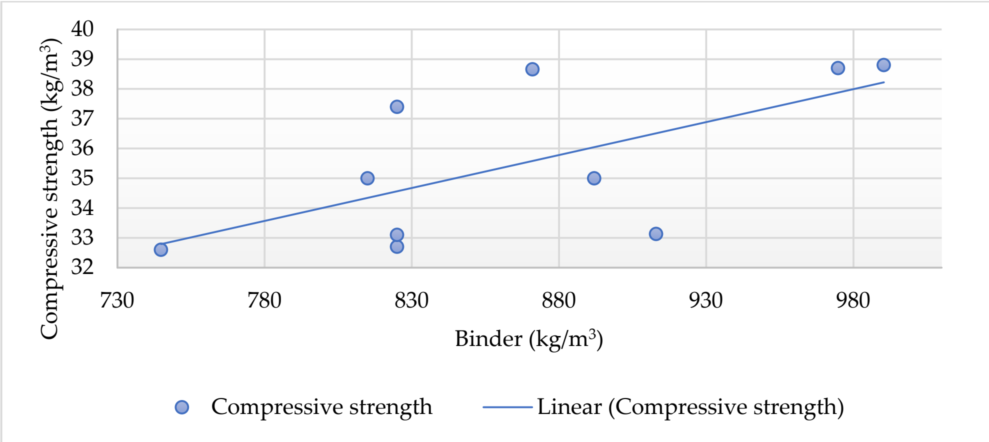


**Figure 6.** Binder vs. compressive strength.

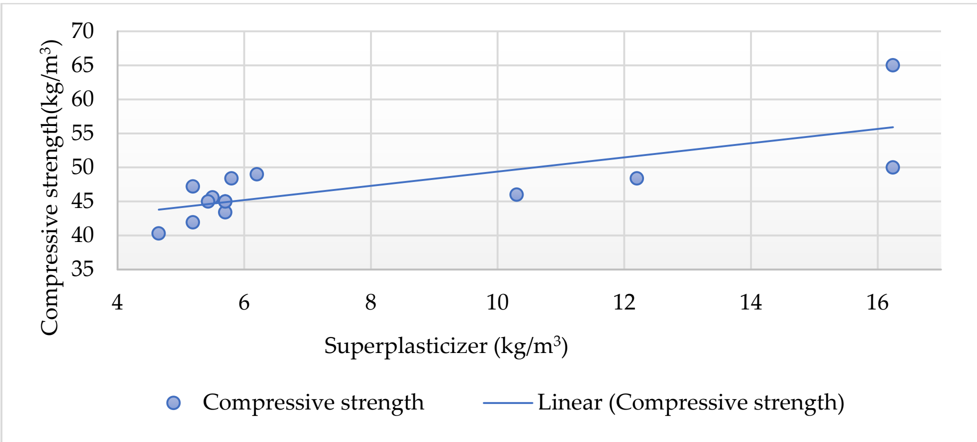


**Figure 7.** Superplasticizer vs. compressive strength.

From the above graph (Figure 6), it is observed that a significant increase in the compressive strength of concrete is achieved by increasing the content of the binder. It is inferred that the binder content can be raised up to 1000 kg/m$^3$.

In Figure 7, it is shown that there is a significant increase in the compressive strength of concrete with an increase in superplasticizer. It is inferred that the superplasticizer dosage is increased to compensate for lost strength. The flexure strength is assessed to find the bending strength of the concrete. It determines the bending compression and bending tension of the concrete. A prism of 40 mm × 40 mm × 160 mm is made and tested for flexure by performing three-point loading. A test block is also made with dimensions of

140 mm × 120 mm × 180 mm to test for flexure in all directions [71]. Anisotropic behavior of the flexure strength is observed by testing the samples in various directions [72].

Unconfined compressive strength is used to find out the shear strength and stability of fresh concrete by making cylinders of 70 mm diameter and 140 mm length, which are tested under a compression testing machine. Cracks are clearly visible in this test [73]. The green strength is established by using this test [74]. It is improved by replacing natural sand with recycled sand [74,75].

Density is the measure of the packing and the level of compaction of the concrete. It is averaged for 100 mm cubes that are made and for the slab specimens with dimensions of 350 mm × 350 mm × 120 mm and 500 mm × 350 mm × 120 mm [68]. Usually, the density varies from 1900 kg/m$^3$ to 2100 kg/m$^3$ depending on the materials used and the compaction procedures [76].

Tensile bond strength plays a major role in 3DCP as there is less reinforcement or none. A direct tension test is conducted by making cylinders with dimensions of 58 mm diameter and 120 mm height. Specimens with dimensions of 100 mm × 100 mm × 500 mm are made in layers to test the same property [68]. Polyethylene (PE) fibres have improved the tensile strength of concrete [77].

The tensile splitting test is another testing procedure used to establish the tensile strength of concrete by making cubes with dimensions of 40 mm × 40 mm × 40 mm and by attaching a wedge to the compression testing machine [78].

Bond shear strength helps in establishing the shear capacity of the concrete when it is printed. In this test, T- and U-shaped moulds are used to determine the bond shear strength. Specimens in three layers with dimensions of 100 mm × 40 mm × 60 mm are made and tested under these moulds [69]. It is found that using polyvinyl alcohol (PVA) fibres improves the shear strength of the concrete.

Porosity is an important parameter that determines the structural packing of the concrete. The helium porosity method is adopted for this, where the cast cubes are kept in an oven at 130 °C for 12 h. Their final weight and volume are noted. Their porosity is established by noting down their bulk volume by means of helium pycnometry [79]. All mechanical properties were compared simultaneously in previous studies [80].

Static yield stress is another important property that is tested. It directly relates to buildability, as a higher value of static yield stress indicates higher buildability, and too high a value of it will stop the flow. It is measured using a Brookfield rheometer in which 450 mL of test material is placed in a 500 mL beaker with a diameter of 95 mm and a depth of 115 mm. It is sheared using a 30 mm × 60 mm vane spindle at a speed of 0.2 s$^{-1}$ for 90 s [81].

## 5. Energy Efficiency of 3DCP

Energy efficiency has become an important factor in the construction industry. It is necessary to make construction sustainable and maintain a thermally comfortable environment. Achieving this with the help of thermal performance is discussed further.

*Thermal Performance*

Thermal performance is a key factor in energy-efficient buildings, where maintaining thermal comfort is essential. It plays a vital role in 3DCP, as walling material constitutes a majority of the structure. A small commercial building model was demonstrated for 3DCP to show its energy-saving potential [82].

Thermal comfort can be improved by reducing the thermal conductivity of the material, which depends on various factors such as aggregate type, porosity of concrete, water-to-cement ratio, and density. Heat transfer can be reduced by using lightweight concrete [83]. The thermal conductivities of concrete in a saturated state have higher values than those of concrete in dry state due to the high heat diffusivity of water [84].

The thermal conductivity of concrete is measured using the steady-state box method, the steady-state hot plate method, and the transient hot wire method. In the steady-state box method, the device contains a hot box and a cold box with concrete inserted between them. The thermal conductivity measurement is achieved by calculating the difference in the air temperature between the boxes. A guarded red-hot plate is used in the steady-state hot plate method, with a concrete sample between two red-hot plates. The rate of heat flow and the temperature difference between them provide a measurement of the thermal conductivity. In the hot wire technique, the thermal conductivity is found by noting down the temperature at a distance from the hot wire.

The usage of GGBS in concrete resulted in a slight increase in the thermal conductivity of the concrete [85]. Fly ash usage in concrete helps in its reduction [86]. The thermal conductivity is reduced when cement is replaced with silica fume [40]. The usage of polyurethane in 3DCP walls reduced energy by 9500 kW per year more than the one without any insulation for a built-up area of 1200 $m^2$ and a wall thickness of 100 mm [87]. To improve the thermal performance of conventional concrete, insulation materials such as expanded polystyrene (EPS), polyurethane, and extruded polystyrene (XPS) with thermal conductivities ranging from 0.02 to 0.04 W/mK are added to the mix [88]. The application of these materials in 3DCP helps in enhancing the thermal performance of the concrete by reducing its thermal conductivity. The usage of phase change materials also helps in reducing the thermal conductivity of the wall [65]. Figure 8 shows the thermal conductivity values of different materials used in the manufacturing of concrete.

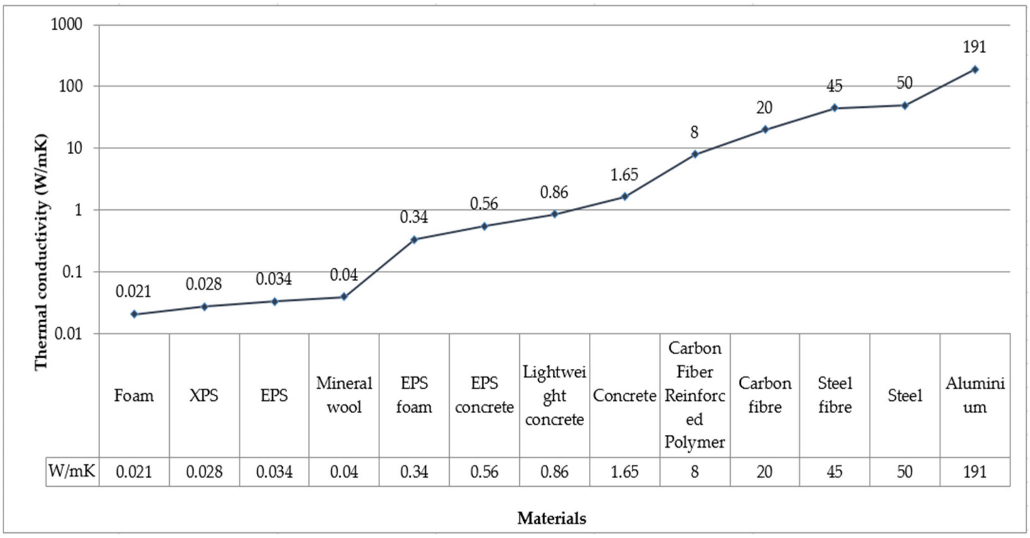


**Figure 8.** Thermal conductivities of different materials used in concrete [88].

Reducing thermal conductivity helps to attain thermal comfort in the structure. This results in a reduction in the cooling load on air conditioners, thereby reducing the electricity consumption and, in turn, lowering the burning of fossil fuels.

## 6. Life Cycle Assessment (LCA) of 3DCP

Life cycle assessment (LCA) is a tool used to discover the environmental impact of product manufacturing from cradle to grave. It helps to identify the sustainability aspect of products [89]. The LCA framework shown in Figure 9 consists of four phases. Defining the goal and scope sets out the intended purpose of study. The life cycle inventory analysis deals with the input of materials used in different stages of construction. The life cycle impact assessment recognizes the potential environmental impacts, and the final stage evaluates the results. Global warming potential is the most assessed indicator, measured in kg $CO_2$ eq., which indicates the carbon footprint of the end product [90]. Three-dimensional concrete printing helps to make sustainable construction [91]. It is an automated construction with less wastage of material, a shorter construction time, and reduced greenhouse gas (GHG) emissions [82]. The additive manufacturing technique, also referred to as 3DCP, constructs the building in layers with high precision and accuracy. It helps in reducing the environmental impact [92]. Cement plays a significant role in the environmental impact of the concrete, which can be reduced by using cement supplements such as GGBS, silica fume, and fly ash [93]. As 3DCP minimizes waste generation to a greater extent, waste treatment of 3DCP is lower than in conventional concrete [94]. Optimizing the distribution of materials reduces the environmental impact by 15% [95].

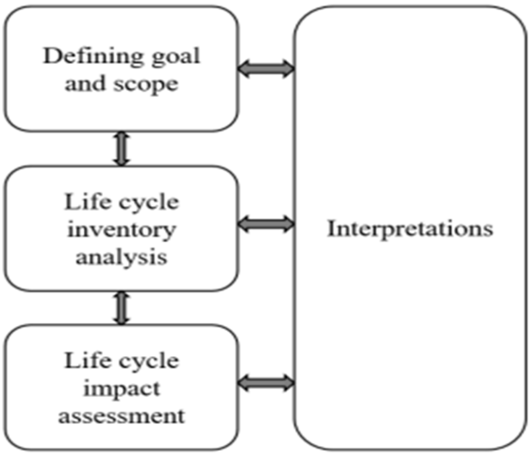


**Figure 9.** Life cycle assessment framework.

## 7. Costing of 3DCPs

Cost is a significant factor to consider in any construction project, and this also applies to 3DCP. The feasibility of 3DCP products is determined by comparing their cost to commercially available products. The cost calculation of 3DCP structures is complex and involves considering various costs in all stages of construction [96]. This includes considering the cost of printing and assembly, which can be higher for 3DCP than for traditional construction methods. The initial cost of 3DCP is generally higher, and the demand for 3DCP products in the market is low. The cost of 3DCP is also affected by social changes, making cost calculation more complicated.

Studies have shown that the cost of prefabricated houses constructed using 3DCP in Japan is 8% higher than that of their available counterparts [97]. However, in Shanghai, a building constructed using 3DCP was more economical than a conventionally constructed building [98]. This inconsistency in cost makes it difficult to determine whether 3DCP is economical or not.

In India, an 1100 sq. ft. building is constructed using 3DCP for a cost of INR 23 lakhs, and various internet sources suggest that 3DCP costs approximately INR 5000–7000 per $m^3$ of concrete. The cost of wall components can be higher due to the cost of printing materials [99], but overall costs can be reduced by minimizing the cost of manpower, as the entire 3DCP process is automated. However, the use of software components can also increase the cost of 3DCP [100].

In conclusion, a clear empirical formula is needed for the accurate cost calculation of 3DCP to determine its economic feasibility compared to traditional construction methods.

## 8. Challenges in 3DCP

As discussed earlier, cost calculation for 3DCP is a major challenge in bringing the technology into the market. A study has shown that shrinkage and cracking are more common in 3DCP, which is a major issue relating to its durability. The active control of rheology is also a major issue for fresh concrete [101]. Anisotropy of 3D concrete is also an issue concerning its structural and long-term durability [102].

Testing 3DCP requires high-cost equipment, and it becomes difficult to analyze the results due to the lack of standard codal provisions. Maintaining the pumpability and buildability of the concrete is relatively difficult when designing the mix proportion. Using thermal insulators such as polyurethane creates difficulty in the availability of materials in the market and thereby a delay in the total project time.

The impact on the environment due to 3DCP technology is comparatively higher than for conventional construction techniques [103]. Developing energy-efficient and low carbon intensive products that reduce the risk to the environment is a challenge. There is a variation in open time and printability for both laboratory-scale and actual site conditions [104].

Due to its high temperature, there is a large evaporation of water from the concrete which leads to cracking of the concrete [105]; this might lead to a reduction in the strength of the concrete.

## 9. Conclusions

From the study, it is concluded that there is a need for the development of 3D concrete with supplementary cementitious materials. This is achieved by replacing cement with GGBS, fly ash, and silica fume. Three-dimensional concrete printing has the potential to achieve faster construction with higher accuracy, better quality, less wastage, and the least usage of manpower. GGBS, fly ash, and silica fume are commonly used as cement substitutes due to their superiority in physico-mechanical properties. As compared to silica fume and fly ash, GGBS has a similar chemical composition to cement. The mixing procedure is performed by fixing the sand/binder ratio, thereby replacing cement with its substitutes. The sand/binder ratio varies from 1.1 to 1.7. The content of the binder is varied from 300 kg/m$^3$ to 1000 kg/m$^3$. The mix with GGBS has a higher compressive and flexure strength as compared to the mix with fly ash and silica fume. Anisotropic behavior of 3DCP is observed in its compressive strength as well as in its flexure strength, which need to be considered carefully when designing the end product. Thermal conductivity plays a key role in establishing the thermal comfort of the structure. Fly ash and silica fume provide better thermal comfort as compared to GGBS. A mix containing polyurethane saves 9500 kW energy as compared to a conventional mix. An LCA study shows that the use of these industrial byproducts can make concrete sustainable. Optimizing the distribution of materials reduces the environmental impact by 15%. As the nozzle plays an important role in the shape stability of the fresh concrete, a screw-type nozzle is preferred for better extrusion of concrete. Efficiency in the design and making process, the capacity of engineers to enable certified elements and building components, and the value of the created components all contribute to the commercial success of 3DCP. Further studies are required in the thermal performance of 3D concrete, as walling components play a vital role in the energy efficiency of structures. Additionally, the development of standards and codal provisions is necessary for 3DCP to be successful commercially.

From the extensive study carried out, it is concluded that using supplementary cementitious materials such as GGBS, fly ash, and silica fume leads to a better performance in the rheological, physical, and mechanical properties of 3D concrete while maintaining the energy efficiency and sustainability of the structure.

**Author Contributions:** Conceptualization, M.S. and R.V.R.; methodology, M.S., S.M., B.A.L., R.C., M.K. and R.V.R.; investigation, M.S. and R.V.R.; writing—original draft preparation, M.S., S.M., B.A.L., R.C. and R.V.R.; writing—review and editing, M.S., S.M., B.A.L., R.C. and R.V.R. All authors have read and agreed to the published version of the manuscript.

**Funding:** This research received no external funding.

**Data Availability Statement:** The data presented in this study are available on request from the corresponding author.

**Conflicts of Interest:** The authors declare no conflict of interest.

## References


1. Schuldt, S.J.; Jagoda, J.A.; Hoisington, A.J.; Delorit, J.D. A Systematic Review and Analysis of the Viability of 3D-Printed Construction in Remote Environments. *Autom. Constr.* **2021**, *125*, 103642. [CrossRef]
2. Panda, B.; Tay, Y.W.D.; Paul, S.C.; Tan, M.J. Current Challenges and Future Potential of 3D Concrete Printing. *Materwiss. Werksttech.* **2018**, *49*, 666–673. [CrossRef]
3. Anjum, T.; Dongre, P.; Misbah, F.; Nanyam, V.P.S.N. Purview of 3DP in the Indian Built Environment Sector. *Procedia Eng.* **2017**, *196*, 228–235. [CrossRef]
4. Roussel, N. Rheological Requirements for Printable Concretes. *Cem. Concr. Res.* **2018**, *112*, 76–85. [CrossRef]
5. Jo, J.H.; Jo, B.W.; Cho, W.; Kim, J.H. Development of a 3D Printer for Concrete Structures: Laboratory Testing of Cementitious Materials. *Int. J. Concr. Struct. Mater.* **2020**, *14*, 13. [CrossRef]
6. Yin, J.; Suo, Y.; Lv, T.; Ma, K.; Wang, X.; Zhang, Z. Application of 3D Printing Technology in the Construction Industry and Its Development Prospects. In Proceedings of the 2021 International Conference on Smart Technologies and Systems for Internet of Things (STS-IOT 2021), Shanghai, China, 17–18 September 2021; Volume 2, pp. 2–8. [CrossRef]
7. Hussein, A.B. Review Paper on 3D Printing Concrete Technology and Mechanics from Industrial Aspect. *Int. J. Eng. Appl. Sci. Technol.* **2021**, *5*, 39–49. [CrossRef]
8. He, L.; Tan, J.Z.M.; Chow, W.T.; Li, H.; Pan, J. Design of Novel Nozzles for Higher Interlayer Strength of 3D Printed Cement Paste. *Addit. Manuf.* **2021**, *48*, 102452. [CrossRef]
9. Xu, J.; Ding, L. *Volume—Forming 3D Concrete Printing Using a Variable—Diameter Square Nozzle*; Budapest University of Technology and Economics: Budapest, Hungary, 2018; pp. 104–113. [CrossRef]
10. Yun, J.-Y.; Jeong, K.-T.; Lee, D. Development of 3D Concrete Extrusion Nozzle for Producing Free-Form Concrete Panels. *Turk. J. Comput. Math. Educ. (TURCOMAT)* **2021**, *12*, 427–436. [CrossRef]
11. Zhang, N.; Sanjayan, J. Extrusion Nozzle Design and Print Parameter Selections for 3D Concrete Printing. *Cem. Concr. Compos.* **2023**, *137*, 104939. [CrossRef]
12. Madurwar, M.V.; Ralegaonkar, R.V.; Mandavgane, S.A. Application of Agro-Waste for Sustainable Construction Materials: A Review. *Constr. Build. Mater.* **2013**, *38*, 872–878. [CrossRef]
13. Madurwar, M.V.; Mandavgane, S.A.; Ralegaonkar, R.V. Development and Feasibility Analysis of Bagasse Ash Bricks. *J. Energy Eng.* **2015**, *141*, 04014022. [CrossRef]
14. Mohamed, O. Durability and Compressive Strength of High Cement Replacement Ratio Self-Consolidating Concrete. *Buildings* **2018**, *8*, 153. [CrossRef]
15. Kamath, M.; Prashant, S.; Kumar, M. Micro-Characterisation of Alkali Activated Paste with Fly Ash-GGBS-Metakaolin Binder System with Ambient Setting Characteristics. *Constr. Build. Mater.* **2021**, *277*, 122323. [CrossRef]
16. Ambroziak, A.; Haustein, E.; Niedostatkiewicz, M. Chemical, Physical, and Mechanical Properties of 95-Year-Old Concrete Built-in Arch Bridge. *Materials* **2021**, *14*, 20. [CrossRef]
17. Rafi, M.M.; Nasir, M.M. Experimental Investigation of Chemical and Physical Properties of Cements Manufactured in Pakistan. *J. Test. Eval.* **2013**, *42*, 774–786. [CrossRef]
18. Zhang, C.; Nerella, V.N.; Krishna, A.; Wang, S.; Zhang, Y.; Mechtcherine, V.; Banthia, N. Mix Design Concepts for 3D Printable Concrete: A Review. *Cem. Concr. Compos.* **2021**, *122*, 104155. [CrossRef]
19. Hou, S.; Xiao, J.; Duan, Z.; Ma, G. Fresh Properties of 3D Printed Mortar with Recycled Powder. *Constr. Build. Mater.* **2021**, *309*, 125186. [CrossRef]
20. Zhang, Y.; Zhang, Y.; Liu, G.; Yang, Y.; Wu, M.; Pang, B. Fresh Properties of a Novel 3D Printing Concrete Ink. *Constr. Build. Mater.* **2018**, *174*, 263–271. [CrossRef]
21. Yu, S.; Xia, M.; Sanjayan, J.; Yang, L.; Xiao, J.; Du, H. Microstructural Characterization of 3D Printed Concrete. *J. Build. Eng.* **2021**, *44*, 102948. [CrossRef]
22. Zhu, B.; Nematollahi, B.; Pan, J.; Zhang, Y.; Zhou, Z.; Zhang, Y. 3D Concrete Printing of Permanent Formwork for Concrete Column Construction. *Cem. Concr. Compos.* **2021**, *121*, 104039. [CrossRef]
23. Panda, B.; Tan, M.J. Experimental Study on Mix Proportion and Fresh Properties of Fly Ash Based Geopolymer for 3D Concrete Printing. *Ceram. Int.* **2018**, *44*, 10258–10265. [CrossRef]
24. Shen, D.; Liu, K.; Wen, C.; Shen, Y.; Jiang, G. Early-Age Cracking Resistance of Ground Granulated Blast Furnace Slag Concrete. *Constr. Build. Mater.* **2019**, *222*, 278–287. [CrossRef]
25. Shen, D.; Jiao, Y.; Gao, Y.; Zhu, S.; Jiang, G. Influence of Ground Granulated Blast Furnace Slag on Cracking Potential of High Performance Concrete at Early Age. *Constr. Build. Mater.* **2020**, *241*, 117839. [CrossRef]
26. Mehta, A.; Siddique, R.; Ozbakkaloglu, T.; Uddin Ahmed Shaikh, F.; Belarbi, R. Fly Ash and Ground Granulated Blast Furnace Slag-Based Alkali-Activated Concrete: Mechanical, Transport and Microstructural Properties. *Constr. Build. Mater.* **2020**, *257*, 119548. [CrossRef]
27. Ramezanianpour, A.A.; Kazemian, A.; Moghaddam, M.A.; Moodi, F.; Ramezanianpour, A.M. Studying Effects of Low-Reactivity GGBFS on Chloride Resistance of Conventional and High Strength Concretes. *Mater. Struct. Mater. Constr.* **2016**, *49*, 2597–2609. [CrossRef]
28. Nath, P.; Sarker, P. Effect of Fly Ash on the Durability Properties of High Strength Concrete. *Procedia Eng.* **2011**, *14*, 1149–1156. [CrossRef]

29. Kesharwani, K.C.; Biswas, A.K.; Chaurasiya, A.; Rabbani, A. Experimental Investigation on Use of Fly Ash in Concrete. *Int. Res. J. Eng. Technol. (IRJET)* **2017**, *4*, 1527–1530.
30. Pati, S.L.; Kale, J.N.; Suman, S. Research Paper fly ash concrete: A technical analysis for. *Int. J. Adv. Eng. Res. Stud.* **2012**, *2*, 128–129.
31. Melichar, J.; Žižková, N.; Brožovský, J.; Mészárosová, L.; Hermann, R. Study of the Interaction of Cement-Based Materials for 3D Printing with Fly Ash and Superabsorbent Polymers. *Buildings* **2022**, *12*, 2008. [CrossRef]
32. Tudjono, S.; Purwanto, X.X.X.; Apsari, K.T. Study the Effect of Adding Nano Fly Ash and Nano Lime to Compressive Strength of Mortar. *Procedia Eng.* **2014**, *95*, 426–432. [CrossRef]
33. Nizar, I.K.; Al Bakri, A.M.M.; Rafiza, A.R.; Kamarudin, H.; Alida, A.; Zarina, Y. Study on Physical and Chemical Properties of Fly Ash from Different Area in Malaysia. *Key Eng. Mater.* **2014**, *594–595*, 985–989. [CrossRef]
34. Bhatt, A.; Priyadarshini, S.; AcharathMohanakrishnan, A.; Abri, A.; Sattler, M.; Techapaphawit, S. Physical, Chemical, and Geotechnical Properties of Coal Fly Ash: A Global Review. *Case Stud. Constr. Mater.* **2019**, *11*, e00263. [CrossRef]
35. Wang, Q.; Shi, M.; Wang, D. Contributions of Fly Ash and Ground Granulated Blast-Furnace Slag to the Early Hydration Heat of Composite Binder at Different Curing Temperatures. *Adv. Cem. Res.* **2016**, *28*, 320–327. [CrossRef]
36. Sharma, A.K.; Sivapullaiah, P.V. Ground Granulated Blast Furnace Slag Amended Fly Ash as an Expansive Soil Stabilizer. *Soils Found.* **2016**, *56*, 205–212. [CrossRef]
37. Sharma, R. Partial Replacement of Cement by Silica Fume. *Int. J. Engg. Dev. Res.* **2018**, *6*, 330–337.
38. Al-Eraky, M.M.; Mohamed, N.; Kamel, F.; Al-Qahtani, A.; Madini, M.A.; Hussin, A.; Kamel, N.M.F. Teaching Professionalism by Vignettes in Psychiatry for Nursing Students. *Int. J. Adv. Res.* **2016**, *4*, 625–634. [CrossRef]
39. Shyam, A.; Anwar, A.; Ahmad, S.A. A Literature Review on Study of Silica Fume as Partial Replacement of Cement in Concrete. *Int. J. Adv. Eng. Manag. Sci.* **2017**, *3*, 250–253. [CrossRef]
40. Srinivas, D.; Dey, D.; Panda, B.; Sitharam, T.G. Printability, Thermal and Compressive Strength Properties of Cementitious Materials: A Comparative Study with Silica Fume and Limestone. *Materials* **2022**, *15*, 8607. [CrossRef] [PubMed]
41. Anisur Rahman, M. Use of Silica Fume in Stabilizing Cement-Dune Sand for Highway Materials. *Am. J. Civ. Eng.* **2017**, *5*, 41. [CrossRef]
42. Nagrockiene, D.; Rutkauskas, A.; Pundiene, I.; Girniene, I. The Effect of Silica Fume Addition on the Resistance of Concrete to Alkali Silica Reaction. *IOP Conf. Ser. Mater. Sci. Eng.* **2019**, *660*, 012031. [CrossRef]
43. Wan Husin, W.N.; Johari, I.; Ibrahim, A.B. Effect of Silica Fume on the Performance of Polyvinyl Alcohol Concrete. *J. Teknol.* **2016**, *78*, 101–106. [CrossRef]
44. Nodehi, M.; Ozbakkaloglu, T.; Gholampour, A. Effect of Supplementary Cementitious Materials on Properties of 3D Printed Conventional and Alkali-Activated Concrete: A Review. *Autom. Constr.* **2022**, *138*, 104215. [CrossRef]
45. Bellum, R.R.; Nerella, R.; Madduru, S.R.C.; Indukuri, C.S.R. Mix Design and Mechanical Properties of Fly Ash and GGBFS-Synthesized Alkali-Activated Concrete (AAC). *Infrastructures* **2019**, *4*, 20. [CrossRef]
46. Prajapati, J.; Karanjit, S. Effect of Coarse Aggregate Sources on the Compressive Strength of Various Grade of Nominal Mixed Concrete. *J. Sci. Eng.* **2019**, *7*, 52–60. [CrossRef]
47. Rehman, A.U.; Kim, J.-H. 3D Concrete Printing: A Systematic Review of Rheology, Mix designs, Mechanical, Microstructural, and Durability Characteristics. *Materials* **2021**, *14*, 3800. [CrossRef]
48. Christen, H.; van Zijl, G.; de Villiers, W. The Incorporation of Recycled Brick Aggregate in 3D Printed Concrete. *Clean. Mater.* **2022**, *4*, 100090. [CrossRef]
49. Khan, M.Z.N.; Shaikh, F.U.A.; Hao, Y.; Hao, H. Effects of Curing Conditions and Sand-to-Binder Ratios on Compressive Strength Development of Fly Ash Geopolymer. *J. Mater. Civ. Eng.* **2018**, *30*, 04017267. [CrossRef]
50. Rao, G.A. Role of Water-Binder Ratio on the Strength Development in Mortars Incorporated with Silica Fume. *Cem. Concr. Res.* **2001**, *31*, 443–447. [CrossRef]
51. Malaeb, Z.; Hachem, H.; Tourbah, A.; Maalouf, T.; El Zarwi, N.; Hamzeh, F. 3D Concrete Printing: Machine and Mix Design. *Int. J. Civ. Eng. Technol.* **2015**, *6*, 14–22.
52. Rahul, A.V.; Santhanam, M.; Meena, H.; Ghani, Z. 3D Printable Concrete: Mixture Design and Test Methods. *Cem. Concr. Compos.* **2019**, *97*, 13–23. [CrossRef]
53. Gupthan, A.S.; Muhsina, S.S.; Reshma, A.; Sharun, M.; Basheerudeen, A. 3d Printinng Concrete: Mix Dessign. *Int. J. Engg. Res. Tech.* **2022**, *11*, 281–284.
54. Lediga, R.; Kruger, D. Optimizing Concrete Mix Design for Application in 3D Printing Technology for the Construction Industry. *Solid State Phenom.* **2017**, *263*, 24–29. [CrossRef]
55. Tay, Y.W.D.; Qian, Y.; Tan, M.J. Printability Region for 3D Concrete Printing Using Slump and Slump Flow Test. *Compos. B Eng.* **2019**, *174*, 106968. [CrossRef]
56. van Overmeir, A.L.; Figueiredo, S.C.; Šavija, B.; Bos, F.P.; Schlangen, E. Design and Analyses of Printable Strain Hardening Cementitious Composites with Optimized Particle Size Distribution. *Constr. Build. Mater.* **2022**, *324*, 126411. [CrossRef]
57. Ding, T.; Xiao, J.; Zou, S.; Yu, J. Flexural Properties of 3D Printed Fibre-Reinforced Concrete with Recycled Sand. *Constr. Build. Mater.* **2021**, *288*, 123077. [CrossRef]
58. Mohan, M.K.; Rahul, A.V.; De Schutter, G.; Van Tittelboom, K. Early Age Hydration, Rheology and Pumping Characteristics of CSA Cement-Based 3D Printable Concrete. *Constr. Build. Mater.* **2021**, *275*, 122136. [CrossRef]

59. Liu, C.; Zhang, R.; Liu, H.; He, C.; Wang, Y.; Wu, Y.; Liu, S.; Song, L.; Zuo, F. Analysis of the Mechanical Performance and Damage Mechanism for 3D Printed Concrete Based on Pore Structure. *Constr. Build. Mater.* **2022**, *314*, 125572. [CrossRef]
60. Zhang, C.; Hou, Z.; Chen, C.; Zhang, Y.; Mechtcherine, V.; Sun, Z. Design of 3D Printable Concrete Based on the Relationship between Flowability of Cement Paste and Optimum Aggregate Content. *Cem. Concr. Compos.* **2019**, *104*, 103406. [CrossRef]
61. Wu, Y.; Liu, C.; Liu, H.; Zhang, Z.; He, C.; Liu, S.; Zhang, R.; Wang, Y.; Bai, G. Study on the Rheology and Buildability of 3D Printed Concrete with Recycled Coarse Aggregates. *J. Build. Eng.* **2021**, *42*, 103030. [CrossRef]
62. Kazemian, A.; Yuan, X.; Cochran, E.; Khoshnevis, B. Cementitious Materials for Construction-Scale 3D Printing: Laboratory Testing of Fresh Printing Mixture. *Constr. Build. Mater.* **2017**, *145*, 639–647. [CrossRef]
63. Muthukrishnan, S.; Ramakrishnan, S.; Sanjayan, J. Technologies for Improving Buildability in 3D Concrete Printing. *Cem. Concr. Compos.* **2021**, *122*, 104144. [CrossRef]
64. Buswell, R.A.; Soar, R.C.; Gibb, A.G.F.; Thorpe, A. Freeform Construction: Mega-Scale Rapid Manufacturing for Construction. *Autom. Constr.* **2007**, *16*, 224–231. [CrossRef]
65. Cui, H.; Yu, S.; Cao, X.; Yang, H. Evaluation of Printability and Thermal Properties of 3D Printed Concrete Mixed with Phase Change Materials. *Energies* **2022**, *15*, 1978. [CrossRef]
66. Amran, M.; Abdelgader, H.S.; Onaizi, A.M.; Fediuk, R.; Ozbakkaloglu, T.; Rashid, R.S.M.; Murali, G. 3D-Printable Alkali-Activated Concretes for Building Applications: A Critical Review. *Constr. Build. Mater.* **2022**, *319*, 126126. [CrossRef]
67. Paul, S.C.; Tay, Y.W.D.; Panda, B.; Tan, M.J. Fresh and Hardened Properties of 3D Printable Cementitious Materials for Building and Construction. *Arch. Civ. Mech. Eng.* **2018**, *18*, 311–319. [CrossRef]
68. Le, T.T.; Austin, S.A.; Lim, S.; Buswell, R.A.; Law, R.; Gibb, A.G.F.; Thorpe, T. Hardened Properties of High-Performance Printing Concrete. *Cem. Concr. Res.* **2012**, *42*, 558–566. [CrossRef]
69. Alchaar, A.S.; Al-Tamimi, A.K. Mechanical Properties of 3D Printed Concrete in Hot Temperatures. *Constr. Build. Mater.* **2021**, *266*, 120991. [CrossRef]
70. Ziejewska, C.; Marczyk, J.; Korniejenko, K.; Bednarz, S.; Sroczyk, P.; Łach, M.; Mikuła, J.; Figiela, B.; Szechyńska-Hebda, M.; Hebda, M. 3D Printing of Concrete-Geopolymer Hybrids. *Materials* **2022**, *15*, 2819. [CrossRef] [PubMed]
71. Pham, L.; Tran, P.; Sanjayan, J. Steel Fibres Reinforced 3D Printed Concrete: Influence of Fibre Sizes on Mechanical Performance. *Constr. Build. Mater.* **2020**, *250*, 118785. [CrossRef]
72. Ye, J.; Cui, C.; Yu, J.; Yu, K.; Xiao, J. Fresh and Anisotropic-Mechanical Properties of 3D Printable Ultra-High Ductile Concrete with Crumb Rubber. *Compos. B Eng.* **2021**, *211*, 108639. [CrossRef]
73. Wolfs, R.J.M.; Bos, F.P.; Salet, T.A.M. Early Age Mechanical Behaviour of 3D Printed Concrete: Numerical Modelling and Experimental Testing. *Cem. Concr. Res.* **2018**, *106*, 103–116. [CrossRef]
74. Ding, T.; Xiao, J.; Qin, F.; Duan, Z. Mechanical Behavior of 3D Printed Mortar with Recycled Sand at Early Ages. *Constr. Build. Mater.* **2020**, *248*, 118654. [CrossRef]
75. Zou, S.; Xiao, J.; Ding, T.; Duan, Z.; Zhang, Q. Printability and Advantages of 3D Printing Mortar with 100% Recycled Sand. *Constr. Build. Mater.* **2021**, *273*, 121699. [CrossRef]
76. Papachristoforou, M.; Mitsopoulos, V.; Stefanidou, M. Evaluation of Workability Parameters in 3D Printing Concrete. *Procedia Struct. Integr.* **2018**, *10*, 155–162. [CrossRef]
77. Zhu, B.; Pan, J.; Nematollahi, B.; Zhou, Z.; Zhang, Y.; Sanjayan, J. Development of 3D Printable Engineered Cementitious Composites with Ultra-High Tensile Ductility for Digital Construction. *Mater. Des.* **2019**, *181*, 108088. [CrossRef]
78. Wolfs, R.J.M.; Bos, F.P.; Salet, T.A.M. Hardened Properties of 3D Printed Concrete: The Influence of Process Parameters on Interlayer Adhesion. *Cem. Concr. Res.* **2019**, *119*, 132–140. [CrossRef]
79. Hambach, M.; Volkmer, D. Properties of 3D-Printed Fiber-Reinforced Portland Cement Paste. *Cem. Concr. Compos.* **2017**, *79*, 62–70. [CrossRef]
80. Meurer, M.; Classen, M. Mechanical Properties of Hardened 3D Printed Concretes and Mortars-Development of a Consistent Experimental Characterization Strategy. *Materials* **2021**, *14*, 752. [CrossRef]
81. Zhang, C.; Deng, Z.C.; Zhang, Y.M.; Chen, C. *Predicting the Yield Stress of 3D Printing Mortar Based on the Flowability of Paste and Excess Paste Thickness*; TU Delft: Delft, The Netherlands, 2021; pp. 674–681.
82. He, Y.; Zhang, Y.; Zhang, C.; Zhou, H. Energy-Saving Potential of 3D Printed Concrete Building with Integrated Living Wall. *Energy Build.* **2020**, *222*, 110110. [CrossRef]
83. Asadi, I.; Shafigh, P.; Abu Hassan, Z.F.B.; Mahyuddin, N.B. Thermal Conductivity of Concrete—A Review. *J. Build. Eng.* **2018**, *20*, 81–93. [CrossRef]
84. Gomes, M.G.; Flores-Colen, I.; Manga, L.M.; Soares, A.; de Brito, J. The Influence of Moisture Content on the Thermal Conductivity of External Thermal Mortars. *Constr. Build. Mater.* **2017**, *135*, 279–286. [CrossRef]
85. Niall, D.; Kinnane, O.; McCormack, S.; West, R.P. Influence of Ground Granulated Blastfurnace Slag on the Thermal Properties of PCM-Concrete Composite Panels. In Proceedings of the Advanced Building Skins Conference, Bern, Switzerland, 10–11 October 2016; pp. 963–973.
86. Kunthe, V.D.; Manavendra, G.; Sondur, V.M. Effect of Thermal Properties on Fly Ash Based Concrete. *Int. Res. J. Eng. Technol. (IRJET)* **2018**, *5*, 396–400.

87. Ayegba, B.O.; Egbe, K.J.I.; Nazar, A.M.; Huang, M.; Hariri-Ardebili, M.A. Resource Efficiency and Thermal Comfort of 3D Printable Concrete Building Envelopes Optimized by Performance Enhancing Insulation: A Numerical Study. *Energies* **2022**, *15*, 1069. [CrossRef]
88. Chippagiri, R.; Bras, A.; Sharma, D.; Ralegaonkar, R.V. Technological and Sustainable Perception on the Advancements of Prefabrication in Construction Industry. *Energies* **2022**, *15*, 7548. [CrossRef]
89. Ram, A.; Sharma, P. A Study on Life Cycle Assessment. *Int. J. Eng. Adv. Technol. (IJEAT)* **2017**, *6*, 197–201.
90. Mahadevan, M.; Francis, A.; Thomas, A. A Simulation-Based Investigation of Sustainability Aspects of 3D Printed Structures. *J. Build. Eng.* **2020**, *32*, 101735. [CrossRef]
91. Alkhalidi, A.; Hatuqay, D. Energy Efficient 3D Printed Buildings: Material and Techniques Selection Worldwide Study. *J. Build. Eng.* **2020**, *30*, 101286. [CrossRef]
92. Chippagiri, R.; Biswal, D.; Mandavgane, S.; Bras, A.; Ralegaonkar, R. Life Cycle Assessment of a Sustainable Prefabricated Housing System: A Cradle-to-Site Approach Based on a Small-Scale Experimental Model. *Buildings* **2023**, *13*, 964. [CrossRef]
93. Tinoco, M.P.; de Mendonça, É.M.; Fernandez, L.I.C.; Caldas, L.R.; Reales, O.A.M.; Toledo Filho, R.D. Life Cycle Assessment (LCA) and Environmental Sustainability of Cementitious Materials for 3D Concrete Printing: A Systematic Literature Review. *J. Build. Eng.* **2022**, *52*, 104456. [CrossRef]
94. Yao, Y.; Hu, M.; Di Maio, F.; Cucurachi, S. Life Cycle Assessment of 3D Printing Geo-Polymer Concrete: An Ex-Ante Study. *J. Ind. Ecol.* **2020**, *24*, 116–127. [CrossRef]
95. Kuzmenko, K.; Gaudillière, N.; Feraille, A.; Dirrenberger, J.; Baverel, O. *Impact: Design with All Senses*; Springer International Publishing: Berlin/Heidelberg, Germany, 2020; ISBN 9783030298296.
96. Yang, H.; Chung, J.K.H.; Chen, Y.; Li, Y. The Cost Calculation Method of Construction 3D Printing Aligned with Internet of Things. *EURASIP J. Wirel. Commun. Netw.* **2018**, *2018*, 147. [CrossRef]
97. Noguchi, M. The Effect of the Quality-Oriented Production Approach on the Delivery of Prefabricated Homes in Japan. *J. Hous. Built Environ.* **2003**, *18*, 353–364. [CrossRef]
98. Wu, P.; Wang, J.; Wang, X. A Critical Review of the Use of 3-D Printing in the Construction Industry. *Autom. Constr.* **2016**, *68*, 21–31. [CrossRef]
99. Buswell, R.A.; Leal de Silva, W.R.; Jones, S.Z.; Dirrenberger, J. 3D Printing Using Concrete Extrusion: A Roadmap for Research. *Cem. Concr. Res.* **2018**, *112*, 37–49. [CrossRef]
100. Pearce, J.M.; Morris Blair, C.; Laciak, K.J.; Andrews, R.; Nosrat, A.; Zelenika-Zovko, I. 3-D Printing of Open Source Appropriate Technologies for Self-Directed Sustainable Development. *J. Sustain. Dev.* **2010**, *3*, 17–29. [CrossRef]
101. De Schutter, G.; Lesage, K.; Mechtcherine, V.; Nerella, V.N.; Habert, G.; Agusti-Juan, I. Vision of 3D Printing with Concrete—Technical, Economic and Environmental Potentials. *Cem. Concr. Res.* **2018**, *112*, 25–36. [CrossRef]
102. Panda, B.; Paul, S.C.; Tan, M.J. Anisotropic mechanical performance of 3D printed fiber reinforced sustainable construction material. *Mater. Lett.* **2017**, *209*, 146–149. [CrossRef]
103. Han, Y.; Yang, Z.; Ding, T.; Xiao, J. Environmental and Economic Assessment on 3D Printed Buildings with Recycled Concrete. *J. Clean Prod.* **2021**, *278*, 123884. [CrossRef]
104. Xiao, J.; Ji, G.; Zhang, Y.; Ma, G.; Mechtcherine, V.; Pan, J.; Wang, L.; Ding, T.; Duan, Z.; Du, S. Large-Scale 3D Printing Concrete Technology: Current Status and Future Opportunities. *Cem. Concr. Compos.* **2021**, *122*, 104115. [CrossRef]
105. Xiao, J.; Lv, Z.; Duan, Z.; Hou, S. Study on Preparation and Mechanical Properties of 3D Printed Concrete with Different Aggregate Combinations. *J. Build. Eng.* **2022**, *51*, 104282. [CrossRef]